Zihim Lam*

Harald Anlauf

Hermann Nirschl

Thin-Film Filtration of Difficult-to-Filter Suspensions Using Polymeric Membranes

Fine-grained particle systems build up a highly consolidated and thin layer on the filter medium and cause a high filter cake resistance. The objective of the novel thin-film filtration process is an effective mechanical separation of these particle systems using membranes on a vacuum drum filter. The mechanical stability of the membrane is evaluated since a roller is required for the cake discharge and the filtration performance is compared with that of a commonly used filter cloth. Analyses reveal that the surface porosity is the crucial factor for the mechanical stability of the membrane. Furthermore, the filter cloth shows a higher filter media resistance than the membrane. A significant increase in the specific dry mass throughput and a particle-free filtrate could be achieved.

1 Introduction

The filtration of fine-grained particles such as microalgae, yeasts, or pigments results in a highly consolidated filter cake with a high specific filter cake resistance. The very dense first cake layer (skin) with its low permeability hinders the subsequent filtration and reduces the efficiency of the filtration process drastically [1, 2]. Low-concentrated suspensions, e.g., fermentation broths and cell homogenisates which are often found in the biotechnology industry, yeast cells and lab ferment which are known from the food industry, or pigments which are used in the chemical industry, even worsen the problem.

The separation of these difficult-to-filter suspensions is still a challenge. Nowadays, several methods are available. However, each separation method comes with disadvantages. A commonly used separation method, e.g., for biological suspensions or fine particles, is centrifugation on the basis of sedimentation [3–5]. Sedimenting centrifuges show high recovery efficiencies, but the low density difference between the biological particles and the surrounding medium as well as the small size of the particles require a rather long sedimentation time. A longer retention time in the bowl leads to high energy requirements of the separation step [3]. Hermeler et al. stated that more than 50 % of the energy consumption in a decanter centrifuge is used for acceleration of the suspension [6]. Flocculation of these particles, in contrast, may show a very low energy requirement, but chemical flocculants are expensive, especially when large volumes of fermentation broths are processed [7]. The recovered products, moreover, are contaminated with the flocculant, which is a problem regarding their application as pharmaceutical products or food.

Another commonly applied method for the separation of difficult-to-filter particle systems is cross-flow filtration or dynamic cross-flow filtration using microporous membranes [8–12]. For example, Rios et al. separated the microalgae *Nannochloropsis* by a one-step harvesting process with dynamic cross-flow filtration. An increase in the concentration from 0.095 to $8 \, \text{g L}^{-1}$ was achieved [13]. Bhave et al. performed two-step harvesting with cross-flow filtration. The suspension with an initial concentration of $0.2 \, \text{g L}^{-1}$ was increased to $150 \, \text{g L}^{-1}$ [14]. However, the further raise in concentration requires a still flowable retentate [15].

In contrast, using a filter press as cake filter would allow to obtain a very dry filter cake. For proper discharge, the filter press, however, requires a thick-enough cake. Since the cake is highly compressible, the filtration time would be very long, and the filtration efficiency would be reduced [16–18]. Another approach is the method of precoat filtration on a vacuum drum filter, where the filter cake is formed on a precoat layer and is scraped off using an advancing knife. This technology, however, comes with other drawbacks, like contamination of the product with precoat material and the additional costs of such substances [19].

A promising novel method for fine-grained particle systems with a high filter cake resistance would be thin-film filtration on a vacuum drum filter using polymeric microporous membranes. Thin-film filtration is based on a short cake filtration time, which has several advantages for the vacuum drum filter. The short filtration time allows the formation of a thin filter

Zihim Lam, Dr. Harald Anlauf, Dr. Hermann Nirschl
Zihim.Lam@kit.edu
Institute of Mechanical Process Engineering and Mechanics (MVM), Karlsruhe Institute of Technology (KIT), Strasse am Forum 8, 76131 Karlsruhe, Germany.

Wiley Online Library

cake with a low absolute filter cake resistance. Especially compressible filter cakes have their maximum flow resistance at the beginning of the filtration process. The highly consolidated cake layer near the surface of the filter medium reduces the efficiency of the subsequent filtration significantly [1, 2]. For this reason, a thin filter cake is favorable. The short cake formation time can be achieved by a higher rotational speed on a vacuum drum filter. This higher rotational speed n can again increase the specific dry mass throughput $\dot{m}_s$ of the vacuum drum filter (Fig. 1) [20, 21].

At the same time, the decreasing filtration time results in a lower cake height h_c. Therefore, common vacuum drum filters have a limited rotational speed n_{max} due to the minimum cake height $h_{c,min}$, which is required for the discharge of the cake (Fig. 1). When employing the usual discharge method on a vacuum drum filter by means of a blade, the filter medium below the filter cake will get damaged if the blade comes too close. For the proper blowback of the filter cake, a minimum filter cake height is also necessary. Another problem is the use of filter cloths, since particularly thin filter cakes would be pressed into the structure of the filter cloths and prevent the complete discharge of the filter cake. These issues result in a minimum cake height of about 5 mm for the discharge.

The novel thin-film filtration method uses polymeric membranes with smooth surfaces and a roller discharger for the complete discharge of thin filter cakes below 1–2 mm. Lam et al. developed a roller discharge method, which allows the discharge of very thin and pasty filter cakes of less than 1 mm from polymeric membranes [22]. The soft roller discharger moves in an opposite direction of drum rotation and can remove the pasty filter cake completely.

Another aspect which comes with the use of membranes on a vacuum drum filter is the cleaning of the installed membranes. To address this problem, Lam et al. developed a method for continuous high-pressure jet cleaning of polymeric membranes on a vacuum drum filter. More than 80 % of the initial throughput of the membrane could be restored for many filter cycles [23]. An impact on the membrane was only detected after 1800 cleaning cycles at a cleaning pressure of 130 bar with 20 filtration steps between each cleaning cycle.

However, for the feasibility of the novel thin-film filtration process using polymeric membranes, two problems need to be clarified. Application requires a sufficient mechanical stability of the membrane to the stress caused by the roller discharger.
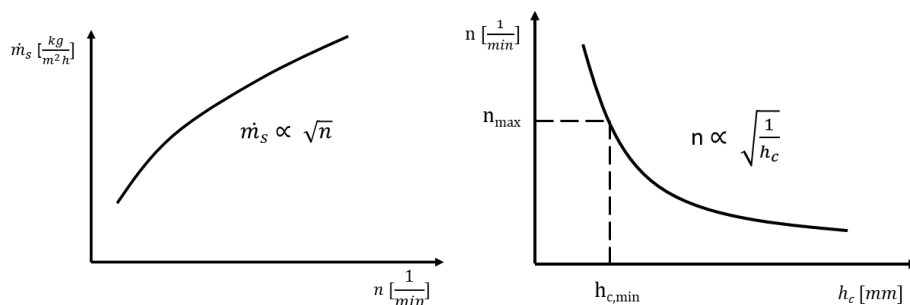
Therefore, the impact of the roller discharger on the membranes with different pore sizes will be examined using a capillary flow porometer.

The change in the pore size distribution is taken as the measure of membrane damage. The pore size distribution before and after mechanical stress has been exerted and will be compared and discussed. Secondly, membranes with fine pores have a much lower liquid throughput than a filter cloth. For this reason, the filtration performance of the polymeric membranes with fine pores needs to be compared to that of the filter cloth with a larger mesh size. The filter medium resistance of a commonly used filter cloth for vacuum drum filters will be compared to the filter medium resistance of the polymeric membrane used here. The results are discussed in relation to the filter cake resistances of the different particle systems. Finally, the specific dry mass throughputs of filter cloth and membrane are investigated and compared using a lab-scale vacuum filter plate.

2 Materials and Methods

2.1 Sample Preparation and Characterization

The first model system is a commercially available wet baker's yeast *Saccharomyces cerevisiae* with a mean particle size of $x_{50,3} = 5.9\,\mu m$ supplied by FALA GmbH (Kehl, Germany). The yeast was suspended in $1\,g\,L^{-1}$ dextrose, 1 mM phosphate buffer, and $1\,g\,L^{-1}$ bacteriological peptone. The dry mass of the yeast suspension was 9.16 wt %. The pH of 6.5 of the suspension was analyzed using a pH meter at a temperature of 20 °C (WTW pH 3310, Xylem Analytics Germany GmbH, Weilheim, Germany). The dry mass was determined after the yeast was dried in an oven for 24 h at a temperature of 90 ± 5 °C.

Titanium dioxide (P90) with a mean particle size of 0.86 μm was purchased from Evonik Degussa GmbH in Germany. The titanium dioxide suspension with a pH of 3.9 had a concentration of 11.46 wt % in a 0.001 M KNO_3 aqueous solution. The particle sizes of all three particle systems were measured with laser diffraction (HELOS/Quixel, Sympatec GmbH, Germany). The dry mass of yeast filter cake was 29.7 wt %, and that of the titanium dioxide filter cake was 75.3 wt % at a gas differential pressure of $\Delta p = 0.8$ bar.

2.2 Filter Medium

The track-etched membranes (PET 0.2/PET 0.4/PET 0.8/PET 1.0) with supporting fibers are made of polyethylene terephthalate (PET; RoTrac, OXYPHEN AG, Wetzikon, Switzerland and Traketch, Sabeu, Northeim, Germany). The images of the membranes were captured by scanning electron microscopy (SEM; S-4500, HITACHI, Japan). In this study, a monofilament nylon filter medium with a mesh

Figure 1. Graphs based on Ehrfeld and Rushton show that the increasing rotational speed n comes with the increase in the specific dry mass throughput $\dot{m}_s$. At the same time, the filter cake height h_c decreases at a higher rotational speed n [20, 21].

opening of 5 µm and a yarn diameter of 37 µm (SEFAR NITEX 03-5/1, SEFAR AG, Heiden, Switzerland) was employed.

2.3 Experimental Setup and Procedure

For investigation of the mechanical stability to the roller discharger, the membranes were installed on a vacuum drum filter. As illustrated in Fig. 2, the roller was pressed onto the membrane using two springs. The two springs caused a line load of $q_P{}^{1)} = 232\,\text{N m}^{-1}$. As indicated in the equation below, the total line load is calculated from the spring rate D, spring travel s, and length L of the roller.

$$q_P = \frac{2Ds}{L} \tag{1}$$

The soft discharge roller with a total diameter of 90 mm and a length of 20 cm has a 5-mm layer of nitrile butadiene rubber with a Shore A hardness of 22°. This soft roller was supplied by Stark Gummiwalzen GmbH (Sontheim, Germany). The vacuum drum has a diameter of 300 mm. According to reference [22], the soft roller moves in the opposite direction of the drum filter to remove the filter cake completely. Therefore, the membranes used for this study were exposed to a mechanical stress where the soft roller and the drum filter moved in an opposite direction.

The pore size distributions of the membranes were investigated using a capillary flow porometer after 1600 rolling cycles (CFP, Porous Materials Inc., Ithaca, USA). The resulting pore size distribution was then compared to that of a new membrane. The target value for comparison is the percentage change in the average pore diameter d_{change}, which is calculated by the average pore diameter d_{before} before the mechanical stress is applied to the membrane and the average pore diameter d_{after} after 1600 rolling cycles:

$$d_{change} = \frac{d_{before} - d_{after}}{d_{before}} \times 100\% \tag{2}$$

The surface porosity Φ_S of each membrane is calculated by the pore density P, the average diameter of the membrane d_{before}, and the area A of 1 cm^2.

$$\Phi_S = \frac{P(d_{before} \times 0.5)^2 \pi}{A} \times 100\% \tag{3}$$

The investigations of the filtration properties were performed in a laboratory filter cell. The filter medium resistance R_m and the specific filter cake resistance r_c were analyzed using a laboratory filter cell with a diameter of 5 cm and a resulting filter area of $A_F = 19.63\,\text{cm}^2$. The filter cake in the laboratory
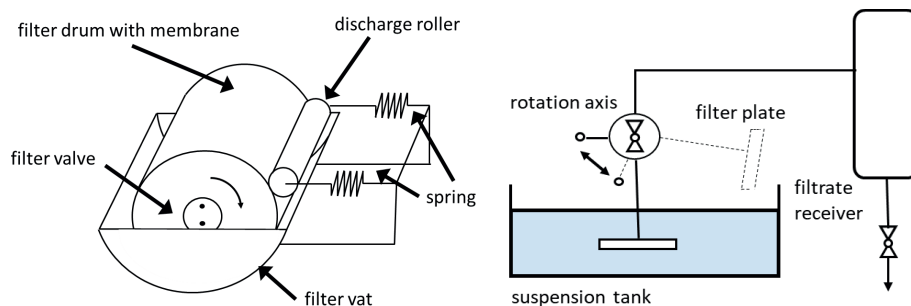

Figure 2. Vacuum drum filter with roller discharger and filter plate.

filter cell was formed at a gas differential pressure of $\Delta p = 0.8$ bar. The equation for the filter medium R_m and the specific filter cake resistance r_c is as follows:

$$\frac{t}{V} = \frac{\eta \kappa}{2(A_F)^2 \Delta p} r_c V + \frac{R_m \eta}{A_F \Delta p} \tag{4}$$

The specific filter cake resistance is calculated from the dynamic viscosity η of the liquid, the concentration parameter κ, the filter area A_F, the gas differential pressure Δp, the filtrate volume V, and the filtration time t. The total filter resistance R_{total} consists of the filter medium resistance R_m and the absolute filter cake resistance R_c.

$$R_{total} = R_c + R_m \tag{5}$$

The absolute filter cake resistance is defined by the filter cake height h_c and the specific filter cake resistance r_c:

$$R_c = r_c h_c \tag{6}$$

The dry mass percentage DM of the filter cake was calculated from the total mass of the wet filter cake m_{tot} and solid mass m_s of the cake after drying at a temperature of 90 ± 5 °C for 24 h.

$$DM = \frac{m_s}{m_{tot}} \times 100\% \tag{7}$$

The filter plate was used to determine the dry mass throughput. The vacuum drum filter showed leakages in the distributor head and reduced the gas differential pressure. Therefore, the actual measured gas differential pressure in the vacuum tank does not represent the gas differential pressure directly on the filter medium. To obtain accurate results, a filter plate was used to ensure a precise gas differential pressure for the filtration. Hence, the specific dry mass throughput $\dot{m}_s$ was determined by a filter plate. The equation to calculate the specific dry mass throughput is:

$$\dot{m}_s = \frac{m_{dry}}{A_P t} \tag{8}$$

The specific dry mass throughput is calculated by the mass of the dry filter cake m_{dry}, the filter area A, and the filtration time t. In general, all cakes were formed for a vacuum of 0.8 bar. For cake filtration, a filter plate with a filter area A_P of $(6 \times 7)\,\text{cm}^2 = 42\,\text{cm}^2$ was selected (Fig. 2). The pressure differ-

---

1)   List of symbols at the end of the paper.

ence on the filter plate was generated by a vacuum pump (UNO 6, Pfeiffer Vacuum GmbH, Asslar, Germany). The rotatable filter plate was submerged into the suspension. After the filter plate was fully immersed in suspension, a gas differential pressure of 0.8 bar was applied by opening the valve. After emerging from the suspension, the filter cakes were manually discharged with a spatula.

Despite the fact that a roller discharger could completely remove the filter cake formed on all of the membranes, the filter cake, which was formed on a filter cloth, could not be completely discharged by the roller discharger. To compare the specific dry mass throughput of the membrane with that of the filter cloth, a manual discharge with a spatula was chosen. The filter cake height was measured by a laser displacement sensor (LK-G157, Keyence Deutschland GmbH, Neu-Isenburg, Germany).

3 Results and Discussion

3.1 Mechanical Stability of the Membrane

Four track-etch membranes with different pore diameters were compared regarding their mechanical stability. For comparison of the membranes, the percentage change in the average pore diameter d_{change} was used as a descriptive parameter. A higher change in the average pore diameter indicates that the pore structure is more affected by the mechanical stress of the roller. A lower change in the average pore diameter means a higher mechanical stability towards the roller discharger.

Fig. 3 displays the pore size distribution of the PET 0.2, PET 0.4, PET 0.8, and PET 1.0 membranes. The pore size distribution of each membrane shows a shift to the left after 1600 rolling cycles, which means that the average pore diameter of the membranes has decreased. The pore size distributions of the PET 0.2, PET 0.4, and PET 0.8 membranes exhibit a significant shift to the left after 1600 rolling cycles on a vacuum
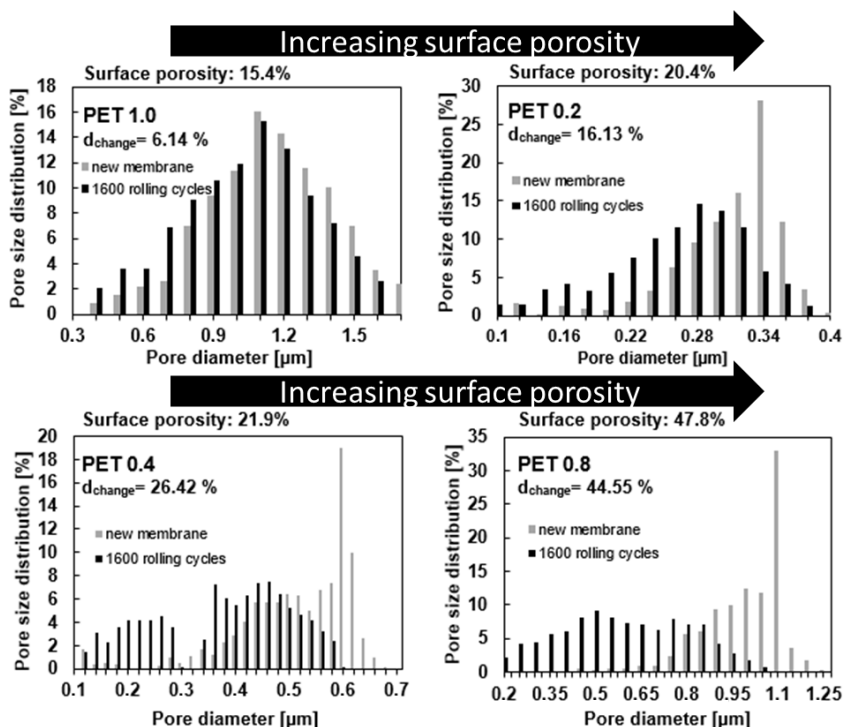

Figure 3. The increasing surface porosity raises the percentage change in the average pore diameter d_{change}.

drum filter. However, the PET 1.0 membrane had a less significant shift to the left. The percentage change in the average pore diameter d_{change} of the PET 1.0 membrane was less than 7 % compared to the other membranes with more than 16 %. A larger average pore diameter d_{before} did not cause a higher percentage change in the average pore diameter d_{change}. Therefore, a relation between the pore diameter of the PET membrane and the percentage change in the average pore diameter could not be observed. As a result, the pore diameter of the membrane does not relate to the mechanical stability to the roller discharge. The properties of each membrane used in the experiments are listed in Tab. 1.

A promising parameter, which can be related to the mechanical stability of the membrane to the roller discharger, is the surface porosity. The PET 1.0 and PET 0.2 membranes with low surface porosities of 15.4 % and 20.4 % show the lowest

Table 1. Properties of each membrane used in the experiments.

Membrane	Rating [μm][a]	d_{before} [μm]	d_{after} [μm][b]	Δd [μm][c]	d_{change} [%][d]	Pore density P [pores/cm²][a]	Surface porosity Φ_S [%]
PET 0.2	0.2	0.31	0.26	0.05	16.13	2.70×10^8	20.38
PET 0.4	0.4	0.53	0.39	0.14	26.42	1.00×10^8	22.06
PET 0.8	0.8	1.1	0.61	0.49	44.55	5.00×10^7	47.52
PET 1.0	1	1.14	1.07	0.07	6.14	1.50×10^7	15.31

[a] Provided by the manufacturer; [b] average pore diameter after 1600 rolling cycles; [c] change in average pore diameter after 1600 rolling cycles; [d] change in the average pore diameter expressed in percentage.

change in the average pore diameter, whereas the PET 0.4 and PET 0.8 membranes with high surface porosities of 21.9 % and 47.8 % have the highest change in the average pore diameters. Fig. 4 demonstrates that the percentage change in the average pore diameter is related to the surface porosity of the membrane and increases with the surface porosity.
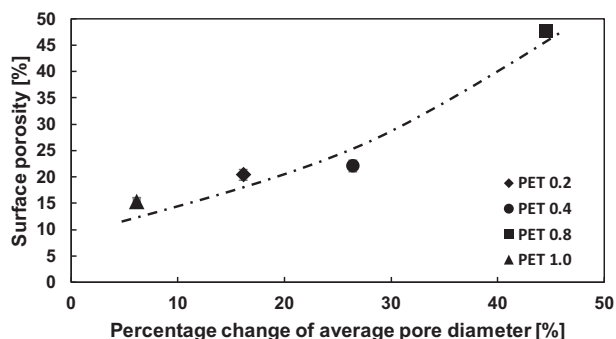

Figure 4. The percentage change in average pore diameter increases with higher surface porosity.

Surface porosity is the main factor for the percentage change in pore diameter and is, therefore, a crucial parameter for the mechanical stability. The pore size distribution of each PET membrane in Fig. 3 reveals that a higher surface porosity results in a more pronounced shift of the pore sizes to the left. The influence of the surface porosity on the change in the pore diameter can be explained as follows. Membranes with a lower surface porosity provide a higher contact surface for the roller. Since the force of the roller is distributed to a higher surface area, the pressure applied to the surface of the membrane per unit area decreases. This results in a lower percentage change in the average pore diameter and, therefore, a higher mechanical stability of the membrane to the roller discharger. Fig. 5 depicts the slight morphological changes of the PET 1.0 membrane after 1600 rolling cycles.
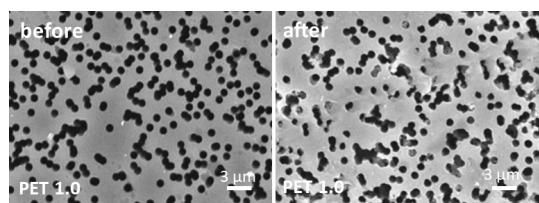

Figure 5. The PET 1.0 membrane only shows a few morphological changes after 1600 rolling cycles.

The results suggest that the right choice of the membrane is important for thin-film filtration due to the mechanical stability towards the roller discharger and is a critical parameter for the feasibility of thin-film filtration.

3.2 Filtration Properties

The feasibility of the PET membrane for thin-film filtration will be tested in the next steps, and the polymeric membrane and the filter cloth will be compared. Consequently, the liquid throughput, filter medium resistance, filter cake resistance, and the specific dry mass throughput will be analyzed. Previous analyses of the mechanical stability of the membranes to the roller discharger reveal that the PET 1.0 membrane exhibits the highest mechanical stability among the investigated membranes. Hence, the PET 1.0 membrane is chosen for further tests of its feasibility and for the comparison with the filter cloth.

The results of the liquid throughput of the PET 1.0 membrane and the filter cloth illustrate that the liquid throughput of the filter cloth Sefar NITEX of $3.96 \times 10^5 \, \mathrm{L\,m^{-2}h^{-1}}$ is much higher than that of the PET 1.0 membrane with $1.33 \times 10^5 \, \mathrm{L\,m^{-2}h^{-1}}$. However, a higher liquid throughput does not necessarily mean a better filtration performance. This will be explained in the following sections.

A high liquid throughput may be a favorable property for the filter medium, but the filter medium resistance and the filter cake resistance are the more crucial parameters for the filtration efficiency. The filter medium resistance is made up of the first layer of the particles on the filter medium and the filter medium itself. Two different particle systems with a comparatively high specific filter cake resistance were selected to analyze the filter medium resistance in a filter cell at a gas differential pressure of $\Delta p = 0.8$ bar. The particle system yeast shows a specific filter cake resistance of $r_c = 2.14 \times 10^{14} \, \mathrm{m^{-2}}$ and the titanium dioxide particles have a specific filter cake resistance of $r_c = 3.35 \times 10^{15} \, \mathrm{m^{-2}}$. The specific filter cake resistances are in the range of 10^{10} to $10^{16} \, \mathrm{m^{-2}}$, where the latter value is considered to represent a very poor filterability.

Fig. 6 compares the filter medium resistance of the filter cloth and the membrane using these two different particle systems. The membrane as well as the filter cloth show a higher filter medium resistance for the titanium dioxide particles. Hence, the particle system affects the filter medium resistance. Fig. 6 also reveals that the filter cloth has a higher filter medium resistance than the polymeric membrane for both particle systems. This phenomenon is due to the longer and highly consolidated particle layers of the particle bridges. At the beginning of filtration, the particles form bridges across the mesh, which lead to the growth of the filter cake.

Fig. 7 presents the larger particle bridges on a filter cloth. The same figure illustrates the shorter particle bridges, which are formed above a membrane. The porosity of these bridges is decisive for the filter medium resistance and is specific for each particle system. The filter medium resistance will increase if the particle bridges become more consolidated and denser. The longer particle bridges on a filter cloth result in a more consolidated structure. This explains the increase in the filter medium resistance for the filter cloth.

In the next step, the filter medium resistance and the absolute filter cake resistance are compared. Ehrfeld [24] mentions that the filter medium resistance can be neglected if it is below about 20 % of the absolute value. The absolute filter cake resistance was calculated by a cake height after a cake filtration time of 5 s. After this time period, yeast particles have formed a cake height of 0.92 mm and the titanium dioxide particles have created a cake height of 0.22 mm. Fig. 6 shows the absolute filter cake resistances of yeast and titanium dioxide. Although the filter cake height of titanium dioxide is much lower than that
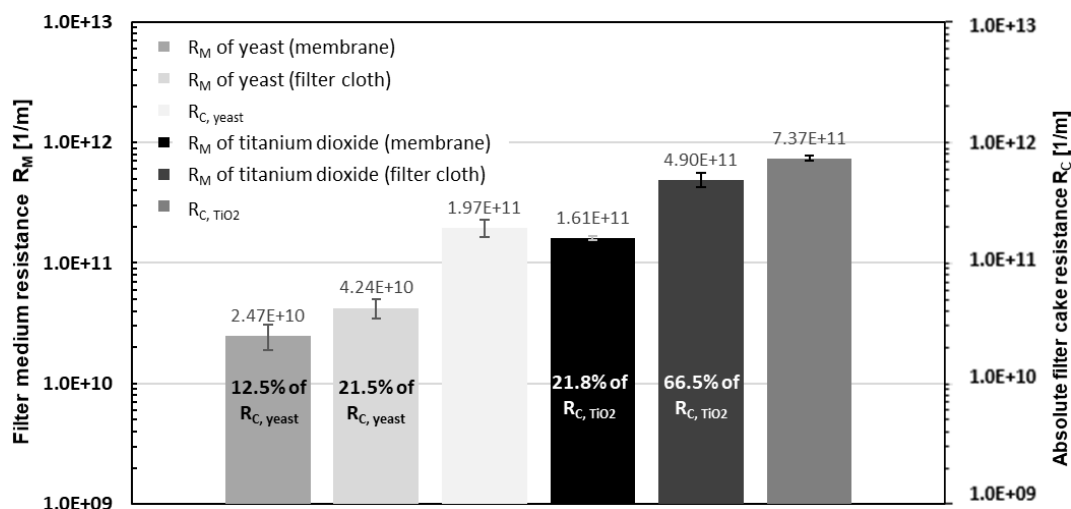
Figure 6. Comparison of absolute filter cake resistances and the filter media resistances of the Sefar NITEX filter cloth and the PET 1.0 membrane.
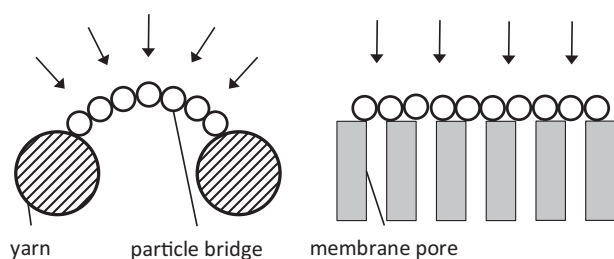

yarn   particle bridge   membrane pore

Figure 7. Large and highly consolidated particle bridges in the filter cloth have a low porosity, which increases the filter medium resistance, whereas membranes have smaller and less consolidated particle bridges.

of yeast, the absolute filter cake resistance is higher because of the higher specific filter cake resistance of the titanium dioxide particles.

The results for yeast in the same figure illustrate that the filter medium resistances of the membrane and the filter cloth are below about 20 % of the absolute filter cake resistance and are negligible. The filter medium resistances of the titanium dioxide particles with a proportion of about 21 % of the absolute filter cake resistance can also be neglected for the membrane, whereas the filter medium resistance of the filter cloth for titanium dioxide particles with a proportion of more than 43 % of the absolute filter cake resistance cannot be neglected. The reason for the increase in the filter medium resistance of the filter cloth is the particle bridges described in the section above. Therefore, using the membrane can even achieve better results for the yeast and titanium dioxide particles than the filter cloth.

Even though the membrane has a much lower liquid throughput than the filter cloth, it turns out that the filtration of particle systems with high specific filter cake resistances is mainly hindered by the filter cake. However, the liquid throughput of a membrane cannot be too low. In this case the bottleneck of the filtration would be located in the membrane itself.

In the next step, the specific dry mass throughput on a filter plate is investigated using the PET 1.0 membrane and the filter cloth with the particle systems titanium dioxide and yeast. The flow resistance of the first cake layer near the filter medium is very high, which slows down the subsequent filtration significantly. Furthermore, the cake porosity increases immensely towards the filter cake surface. As a result, the subsequent filtration occurs with slower and with a lower dry mass. For this reason, further filtration is inefficient, and a thin filter cake needs to be discharged to maintain a high filtration efficiency. Common minimum filter cake heights, which can still be discharged on a filter cloth, are above 2 mm. Therefore, the specific dry mass throughput of the vacuum drum filter using a filter cloth is limited.

The filter plate is a suitable filtration device for upscale of a vacuum drum filter and represents a filter cell on the vacuum drum filter. The reduction in filtration time on a filter plate is equivalent to the increase in rotational speed on a vacuum drum filter. The results obtained for the filter plate reveal that the filtration time of about 20 s and a gas differential pressure of $\Delta p = 0.8$ bar corresponds to a filter cake height of 1.8 mm for yeast (Fig. 8a). The specific dry mass throughput for yeast at a filtration time of 20 s is 106 kg m^{-2}h^{-1} (Fig. 8b).

Once the filtration time decreases to 5 s, the filter cake has a height of 0.92 mm and a specific dry mass throughput of 225 kg m^{-2}h^{-1}. Hence, the thin-film filtration using polymeric membranes could enhance the specific dry mass throughput significantly. Both the filter cloth and the polymeric membrane show the same specific dry mass throughputs for yeast. Therefore, the polymeric membrane is not less efficient than the filter cloth although it has a much lower liquid throughput than the filter cloth. Though the specific dry mass throughput of the filter cloth and the membrane are similar, the important advantage of the polymeric membrane is the complete discharge using a roller. To compare the filter cloth and the polymeric membrane, the discharge for these set of experiments was carried out manually. The dry mass of the filter cake of the yeast cells formed on a membrane and a filter cloth were also in the
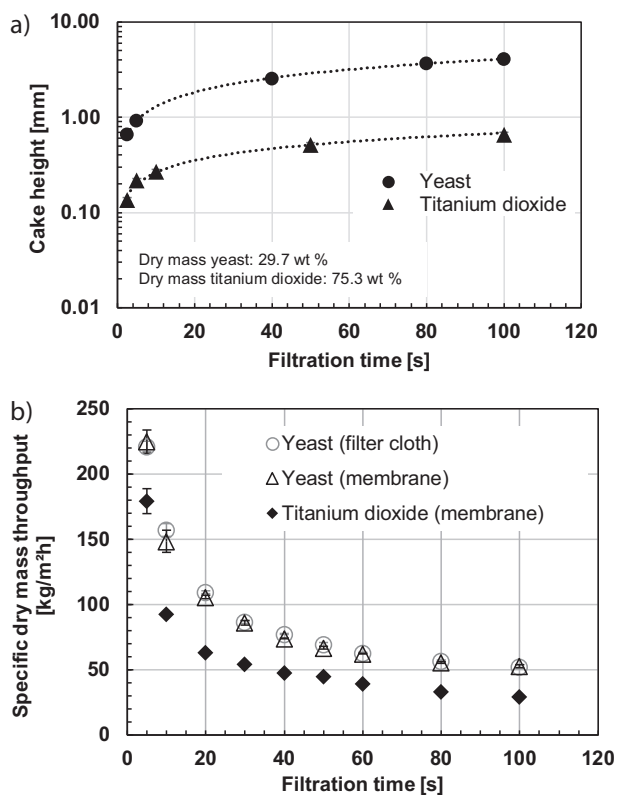
Figure 8. (a) Filter cake heights of yeast and titanium dioxide; (b) specific dry mass throughput on a filter plate using a membrane and a filter cloth at a gas differential pressure of $\Delta p = 0.8$ bar.

film filtration can also prevent product loss or a cost-intensive secondary clarification of the turbid filtrate.

4 Conclusions

Analysis of the mechanical stability of PET membranes reveals that the surface porosity is the decisive factor for the percentage change of the average pore size. The increase in surface porosity resulted in a higher percentage change of the average pore diameter and therefore a lower mechanical stability. It was also found that the pore diameter of the membrane is not a significant parameter for determining the mechanical stability towards the roller discharger.

The PET 1.0 membrane with the lowest surface porosity was found to be barely affected by the roller discharger. The comparison of the filtration properties of this polymeric membrane and the filter cloth reveals that even though the membrane has a much lower liquid throughput than the filter cloth, the filtration performance is not affected. The relevant filter medium resistance of this membrane is actually lower than that of the filter cloth due to the particle bridges.

Experimental results on the filter plate illustrate that the specific dry mass throughput of the membrane and the filter cloth are in the same range. A further increase in the specific dry mass throughput on a vacuum drum filter is limited by a minimum cake height because of the filter cloth. The thin-film filtration on a vacuum drum filter enables an increase in the rotational speed by using membranes and a roller discharger. It allows to go beyond the maximum rotational speed and enhances the specific dry mass throughput significantly. Difficult-to-filter suspensions are often low-concentrated and have a high filter cake resistance at the same time, which leads to the formation of a highly consolidated thin layer. Thin-film filtration using polymeric membranes was found to be a promising and efficient method for difficult-to-filter suspensions.

Acknowledgment

The authors have declared no conflict of interest.

same range of about 30 wt %. The much lower dry mass compared to that of the titanium dioxide particles is due to the intracellular liquid inside the yeast cells.

The particle system titanium dioxide shows a filter cake height of less than 1 mm for a filtration time of 100 s. The specific dry mass throughput for this filtration time is $29 \, \text{kg} \, \text{m}^{-2} \text{h}^{-1}$. The reduction in the filtration time to 5 s can boost the specific dry mass throughput to more than $180 \, \text{kg} \, \text{m}^{-2} \text{h}^{-1}$. For this particle system, comparable values of titanium dioxide using the filter cloth could not be measured, because one part of the filter cake remained in the filter cloth during the discharge.

To compare the filter cloth and the membrane, all filter cakes were discharged manually. However, even the manual discharge of the titanium dioxide filter cake could not remove the filter cake completely from the filter cloth. Hence, Fig. 8b only displays the results of the specific dry mass throughput of the titanium dioxide particles using a polymeric membrane. The results on the filter plate demonstrate that especially highly compressible particle systems with consolidated thin cake layers can be efficiently separated by means of thin-film filtration with polymeric membranes.

Additionally, thin-film filtration using membranes has a particle-free and clear filtrate for the tested particle systems. The filtrate of the polymeric membrane is clear, whereas the filter cloth filtrate is turbid for both particle systems. Hence, thin-

Symbols used

A_F	[m²]	filter area of the filter cell
A_P	[m²]	filter area of the filter plate
D	[N m⁻¹]	spring rate
DM	[%]	dry mass
d	[μm]	pore diameter
h_c	[mm]	cake height
L	[mm]	length of the roller
m_s	[g]	specific mass of the dry filter cake
$\dot{m}_s$	[kg h⁻¹m⁻²]	specific dry mass throughput
m_{tot}	[g]	total mass of the wet filter cake

n	[min^{-1}]	rotational speed
Δp	[N m^{-2}]	gas differential pressure
P	[cm^{-2}]	pore density
q_P	[N m^{-1}]	line load
r_c	[m^{-2}]	specific filter cake resistance
R_c	[m^{-1}]	absolute filter cake resistance
R_m	[m^{-1}]	filter medium resistance
s	[mm]	spring travel
t	[s]	filtration time
V	[cm^3]	filtrate volume

Greek letters

η	[N s m^{-2}]	dynamic viscosity
κ	[–]	concentration coefficient
Φ_S	[%]	surface porosity

Sub- and superscripts

after	average pore diameter after mechanical stress
before	average pore diameter before mechanical stress
change	difference in pore diameter before and after mechanical stress
c,min	minimum cake height
max	maximum rotational speed

Abbreviations

PES	polyethersulfone
PET	polyethylene terephthalate
SEM	scanning electron microscopy

References

[1] T. Mattsson, M. Sedin, H. Theliander, Filtration Properties and Skin Formation of Micro-crystalline Cellulose, *Sep. Purif. Technol.* **2012**, *96*, 139–146. DOI: https://doi.org/10.1016/j.seppur.2012.05.029

[2] S. S. Yim, Y. M. Song, Porosity Distribution in Highly Compressible Cake: Experimental and Theoretical Verification of the Dense Skin, *Korean J. Chem. Eng.* **2008**, *25 (6)*, 1524–1531. DOI: https://doi.org/10.1007/s11814-008-0251-7

[3] A. J. Dassey, C. S. Theegala, Harvesting Economics and Strategies Using Centrifugation for Cost Effective Separation of Microalgae Cells for Biodiesel Applications, *Bioresour. Technol.* **2013**, *128*, 241–245. DOI: https://doi.org/10.1016/j.biortech.2012.10.061

[4] L. E. Spelter, A. Steinwand, H. Nirschl, Processing of Dispersions Containing Fine Particles or Biological Products in Tubular Bowl Centrifuges, *Chem. Eng. Sci.* **2010**, *65 (14)*, 4173–4181. DOI: https://doi.org/10.1016/j.ces.2010.04.028

[5] M. Konrath, M. Hackbarth, H. Nirschl, Process Monitoring and Control for Constant Separation Conditions in Centrifugal Classification of Fine Particles, *Adv. Powder Technol.* **2014**, *25 (3)*, 991–998. DOI: https://doi.org/10.1016/j.apt.2014.01.022

[6] J. Hermeler, L. Horstkötter, T. Hartmann, Neue Dekantergeneration mit verbessertem energetischen Wirkungsgrad, *F&S, Filtr. Sep.* **2012**, *26 (3)*, 158–166.

[7] D. Vandamme, I. Foubert, I. Fraeye, B. Meesschaert, K. Muylaert, Flocculation of *Chlorella vulgaris* Induced by High pH: Role of Magnesium and Calcium and Practical Implications, *Bioresour. Technol.* **2012**, *105*, 114–119. DOI: https://doi.org/10.1016/j.biortech.2011.11.105

[8] S. Ripperger, J. Altmann, Crossflow Microfiltration – State of the Art, *Sep. Purif. Technol.* **2002**, *26 (1)*, 19–31. DOI: https://doi.org/10.1016/S1383-5866(01)00113-7

[9] N. Rossignol, L. Vandajon, P. Jaouen, F. Quemeneur, Membrane Technology for the Continuous Separation Microalgae/Culture Medium: Compared Performances of Crossflow Microfiltration and Ultrafiltration, *Aquac. Eng.* **1991**, *20 (3)*, 191–208. DOI: https://doi.org/10.1016/S0144-8609(99)00018-7

[10] I. H. Huisman, D. Elzo, E. Middelink, A. C. Tragardh, Properties of the Cake Layer Formed during Crossflow Microfiltration, *Colloids Surf., A* **1998**, *138*, 265–281. DOI: https://doi.org/10.1016/S0927-7757(96)03976-3

[11] R. Bott, T. Langeloh, E. Ehrfeld, Dynamic Cross Flow Filtration, *Chem. Eng. J.* **2000**, *80 (1–3)*, 245–249. DOI: https://doi.org/10.1016/S1383-5866(00)00097-6

[12] S. S. Lee, S. Burt, G. Russotti, B. Buckland, Microfiltration of Recombinant Yeast Cells Using a Rotating Disk Dynamic Filtration System, *Biotechnol. Bioeng.* **1995**, *48*, 386–400. DOI: https://doi.org/10.1002/bit.260480411

[13] S. D. Rios, J. Salvado, X. Farriol, C. Torras, Antifouling Microfiltration Strategies to Harvest Microalgae for Biofuel, *Bioresour. Technol.* **2012**, *119*, 406–418. DOI: https://doi.org/10.1016/j.biortech.2012.05.044

[14] R. Bhave, T. Kuritz, L. Powell, D. Adcock, Membrane-Based Energy Efficient Dewatering of Microalgae in Biofuels Production and Recovery of Value Added Co-products, *Environ. Sci. Technol.* **2012**, *46*, 5599–5606. DOI: https://doi.org/10.1021/es204107d

[15] H. Anlauf, A. Erk, Continuous "Skin" Filtration of Very Difficult-to-Filter Suspensions, *Aufbereit.-Tech.* **2006**, *47 (3)*, 22–29.

[16] A. D. Stickland, R. G. de Kretser, P. J. Scales, S. P. Usher, P. Hillis, M. R. Tillotson, Numerical Modelling of Fixed-Cavity Plate-and-Frame Filtration: Formulation, Validation and Optimisation, *Chem. Eng. Sci.* **2006**, *61 (12)*, 3818–3829. DOI: https://doi.org/10.1016/j.ces.2006.01.020

[17] K. A. Landman, L. R. White, Predicting Filtration Time and Maximizing Throughput in a Pressure Filter, *AlChE J.* **2004**, *43 (12)*, 3147–3160. DOI: https://doi.org/10.1002/aic.690431204

[18] A. D. Stickland, R. G. de Kretser, A. R. Kilcullen, P. J. Scales, P. Hillis, M. R. Tillotson, *AIChE J.* **2008**, *54 (2)*, 464–474. DOI: https://doi.org/10.1002/aic.11369

[19] C. Boittelle, C. Poupot, V. Milisic, M. Mietton-Peuchot, Advances in the Precoat Filtration Process, *Sep. Sci. Technol.* **2008**, *43 (7)*, 1701–1712. DOI: https://doi.org/10.1080/01496390801974563

[20] E. Ehrfeld, Faustformeln und Merksätze, *CITplus* **2003**, *6 (11)*, 20–22.

[21] A. Rushton, Pressure Variation Effects in Rotary Drum Filtration with Incompressible Cakes, *Powder Technol.* **1978**, *20 (1)*, 39–46. DOI: https://doi.org/10.1016/0032-5910(78)80006-0

[22] Z. Lam, H. Anlauf, H. Nirschl, Roller Discharge of Thin Film Filter Cakes from Membranes: A Key to the Thin Film Filtration, *Sep. Purif. Technol.* **2019**, *221*, 38–43. DOI: https://doi.org/10.1016/j.seppur.2019.03.062

[23] Z. Lam, H. Anlauf, H. Nirschl, High-Pressure Jet Cleaning of Polymeric Microfiltration Membranes, *Chem. Eng. Tech-* *nol.* **2019**, *43 (3)*, 457–464. DOI: https://doi.org/10.1002/ceat.201900449

[24] E. Ehrfeld, Influence of Filter Cloth Behavior on the Layout of Cake Forming Filters, *Chem. Eng. Technol.* **2010**, *33 (8)*, 1349–1357. DOI: https://doi.org/10.1002/ceat.201000135